Supplemental Material for "Microvascular basis for growth of small infarcts following occlusion of single penetrating arterioles in mouse cortex" by Zachary J. Taylor, Edward S. Hui, Ashley N. Watson, Xingju Nie, Rachael L. Deardorff, Jens H. Jensen, Joseph A. Helpern and Andy Y. Shih

Figure S1. Comparison of vasodynamic parameters between mouse and rat penetrating vessels. (A) Scatter plot and histograms of centerline RBC velocity, v(0), plotted as a function of lumen diameter, d, for individual penetrating arterioles from mouse (red, this study) and rat[17] (black). The mean ± SEM for all data points in each group are shown adjacent to the histogram. **(B)** Histogram showing the distribution of RBC volume flux, F, for penetrating arterioles from mouse (red) and rat[17] (black). A vertical line marks the average flux for each species and the range for SEM is shaded. **(C, D)** Equivalent plots of panels A and B for mouse (blue) and rat (black) penetrating venules. Note the different x and y scales for panels A and C.

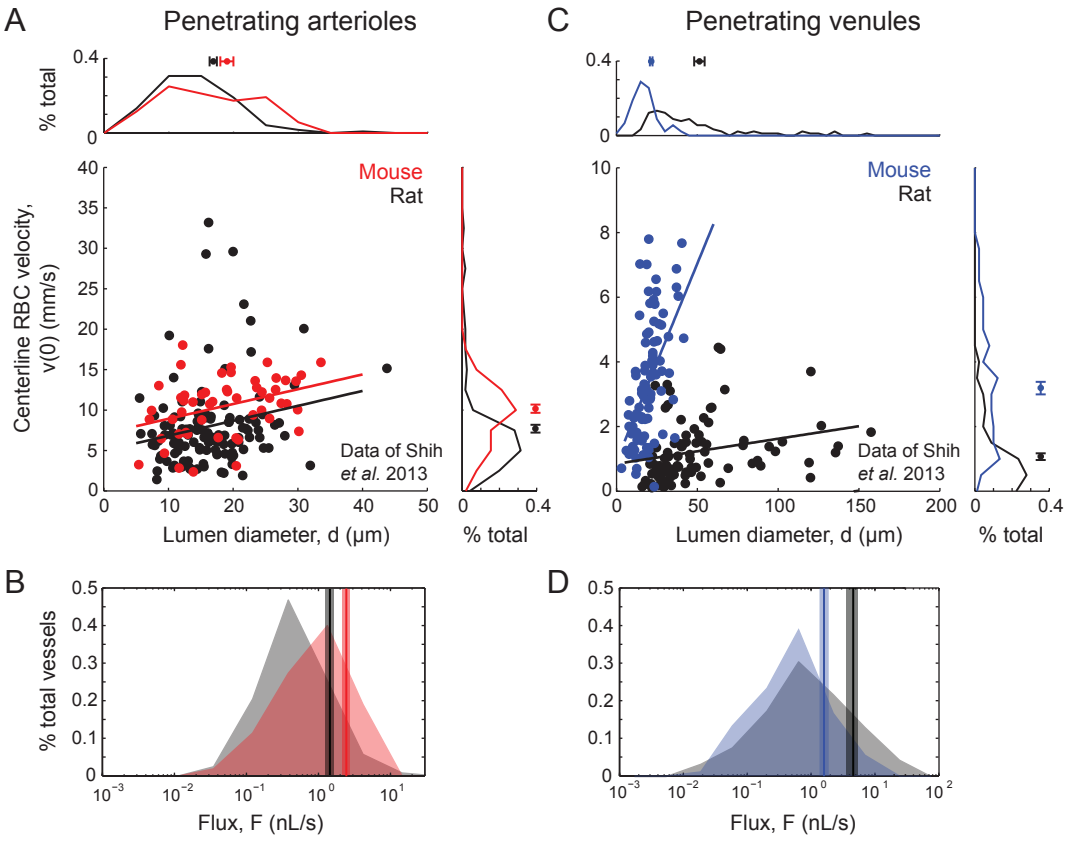

Figure S1. Taylor, Hui, Watson, Nie, Deardorff, Jensen, Helpern and Shih

Supplemental Material for "Microvascular basis for growth of small infarcts following occlusion of single penetrating arterioles in mouse cortex " by Zachary J. Taylor, Edward S. Hui, Ashley N. Watson, Xingju Nie, Rachael L. Deardorff, Jens H. Jensen, Joseph A. Helpern and Andy Y. Shih

Figure S2. Comparison of computed penetrating arteriole perfusion domains with measured infarct volumes. Infarct volumes resulting from the photothrombotic occlusion of individual penetrating arterioles (red circles, derived from Fig. 2D, right panel) plotted as a function of pre-occlusion flux. This was further overlaid with the computed vascular perfusion domains and their estimated parenchymal volume gathered from analyses of large-scale vascular reconstructions from C57Bl/6 mouse cortex (gray circles)[24].

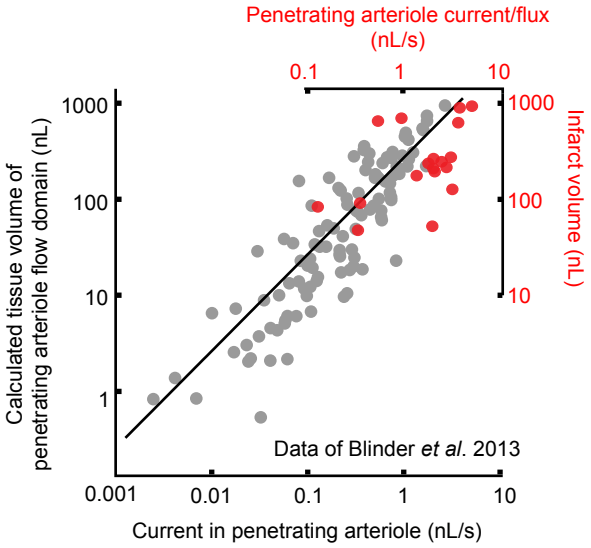

Figure S2. Taylor, Hui, Watson, Nie, Deardorff, Jensen, Helpern and Shih

Supplemental Material for "Microvascular basis for growth of small infarcts following occlusion of single penetrating arterioles in mouse cortex " by Zachary J. Taylor, Edward S. Hui, Ashley N. Watson, Xingju Nie, Rachael L. Deardorff, Jens H. Jensen, Joseph A. Helpern and Andy Y. Shih

Figure S3. Capillary flow in tissues proximal and distal to targeted penetrating arterioles. (A) Wide-field two-photon image showing the location of high-resolution imaging (magenta square, center of image stack 0 to 350 μm from target arteriole) relative to an occluded penetrating arteriole (green circle). A more distant control region was also sampled (yellow square, center of image stack 350 to 500 μm from target arteriole), which was located just outside the border of the eventual infarct (dotted line). **(B)** Compared to the tissue region sampled near the targeted penetrating arteriole (199 capillaries from 4 infarcts), capillaries in the distant control region (173 capillaries from 3 infarcts) retain significantly more flow over the duration of the imaging experiment.

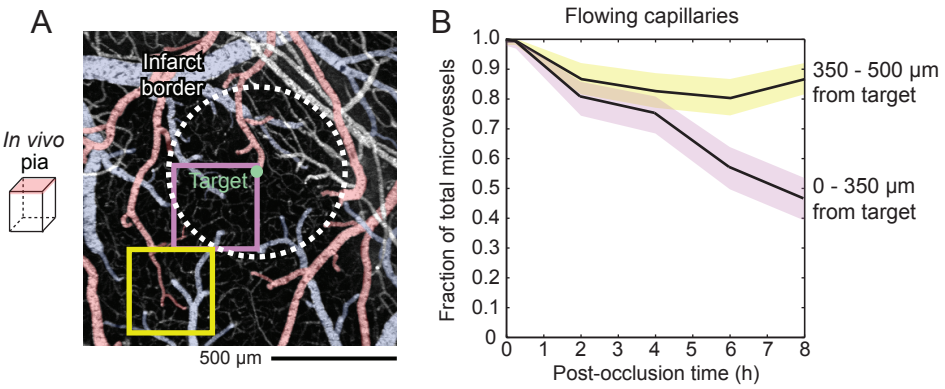

Figure S3. Taylor, Hui, Watson, Nie, Deardorff, Jensen, Helpern and Shih

Supplemental Material for "Microvascular basis for growth of small infarcts following occlusion of single penetrating arterioles in mouse cortex " by Zachary J. Taylor, Edward S. Hui, Ashley N. Watson, Xingju Nie, Rachael L. Deardorff, Jens H. Jensen, Joseph A. Helpern and Andy Y. Shih

Figure S4. Constrictive and dilative responses of capillaries in the stroke periphery. (A) Absolute lumen diameters of capillaries that constricted by 20% or more of baseline, plotted as a function of time post-occlusion. **(B)** Data of panel A normalized to pre-occlusion lumen diameter. **(C, D)** Equivalent data of panels A and B for microvessels that dilated by 20% or more of baseline. Mean ± SEM is shown for each panel as a black line with gray shading.

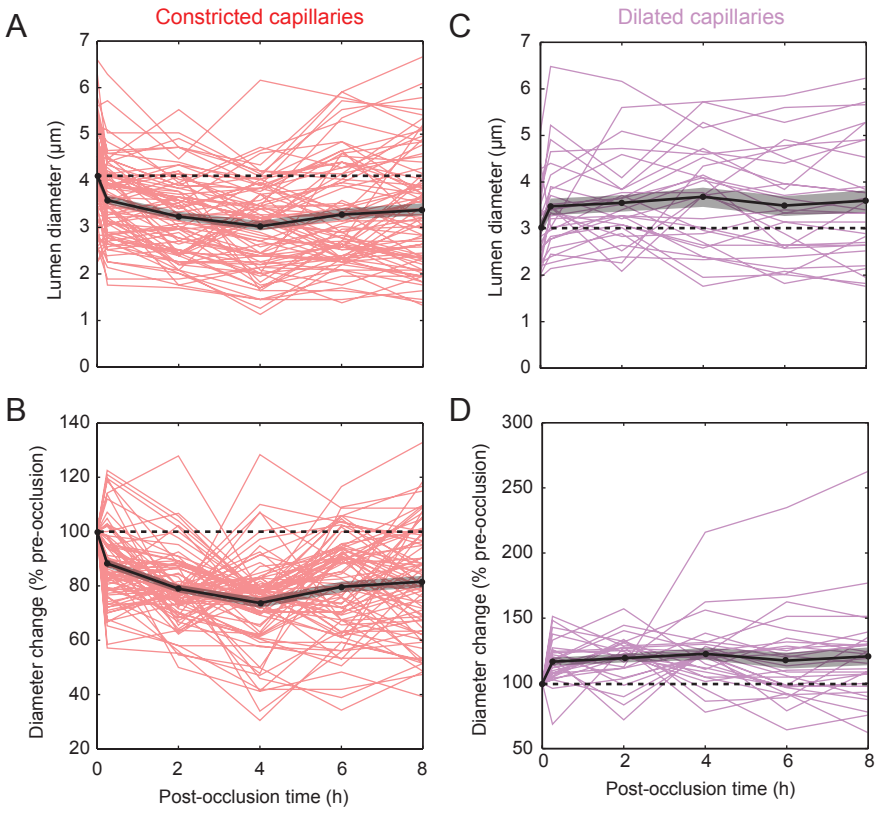

Figure S4. Taylor, Hui, Watson, Nie, Deardorff, Jensen, Helpern and Shih

Supplemental Material for "Microvascular basis for growth of small infarcts following occlusion of single penetrating arterioles in mouse cortex " by Zachary J. Taylor, Edward S. Hui, Ashley N. Watson, Xingju Nie, Rachael L. Deardorff, Jens H. Jensen, Joseph A. Helpern and Andy Y. Shih

Figure S5. Off-target occlusions induce capillary dilation rather than constriction. (A) Wide-field two-photon image showing the location of high-resolution imaging of capillaries (cyan squares) relative to the location of an off-target surface arteriole occlusion (green circle). **(B)** A magnified image (yellow square from panel A) showing the site of occlusion (green circle) in relation to a typical penetrating arteriole that would be occluded for on-target experiments (yellow arrowhead). **(C)** Cumulative distribution plot of change in capillary diameter following off-target occlusions (black) and on-target penetrating arteriole occlusions (red). Note the shift toward dilation for off-target occlusions ($p < 0.001$, Kolmogorov-Smirnov test, $n = 118$ capillaries from 2 mice for off-target occlusions and $n = 94$ capillaries from 2 mice for on-target occlusions). **(D)** Proportion of capillaries that changed significantly in diameter, constriction or dilation, in off-target and on-target experiments. Error bars represent 0.95 confidence intervals.

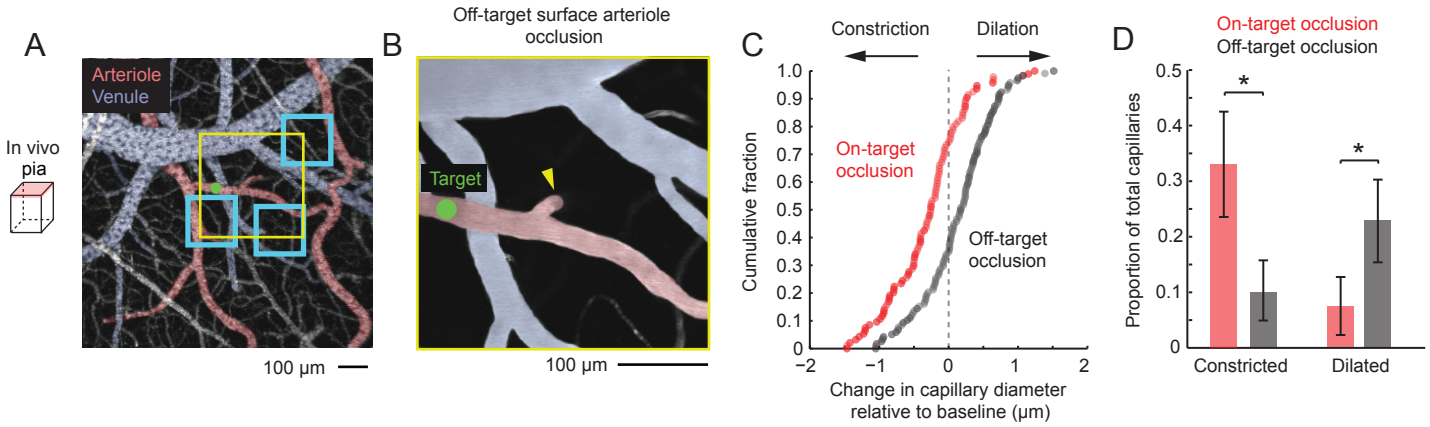

Figure S5. Taylor, Hui, Watson, Nie, Deardorff, Jensen, Helpern and Shih

Supplemental Material for "Microvascular basis for growth of small infarcts following occlusion of single penetrating arterioles in mouse cortex " by Zachary J. Taylor, Edward S. Hui, Ashley N. Watson, Xingju Nie, Rachael L. Deardorff, Jens H. Jensen, Joseph A. Helpern and Andy Y. Shih

Figure S6. Platelet aggregation in capillaries of the infarct and immediate peri-infarct. Triple-label immunohistochemistry for green FITC-dextran retention (indicative of BBB damage), white collagen IV (microvascular basement membrane), and red CD41 (platelets) on an infarct captured at 4 hours (upper row) and 24 hours post-occlusion (lower row). Note the strong spatial link between platelet aggregation and FITC-dextran in ischemia-damaged capillaries, but not all capillaries. This suggests that capillary thrombosis was involved in flow stagnation and BBB leak.

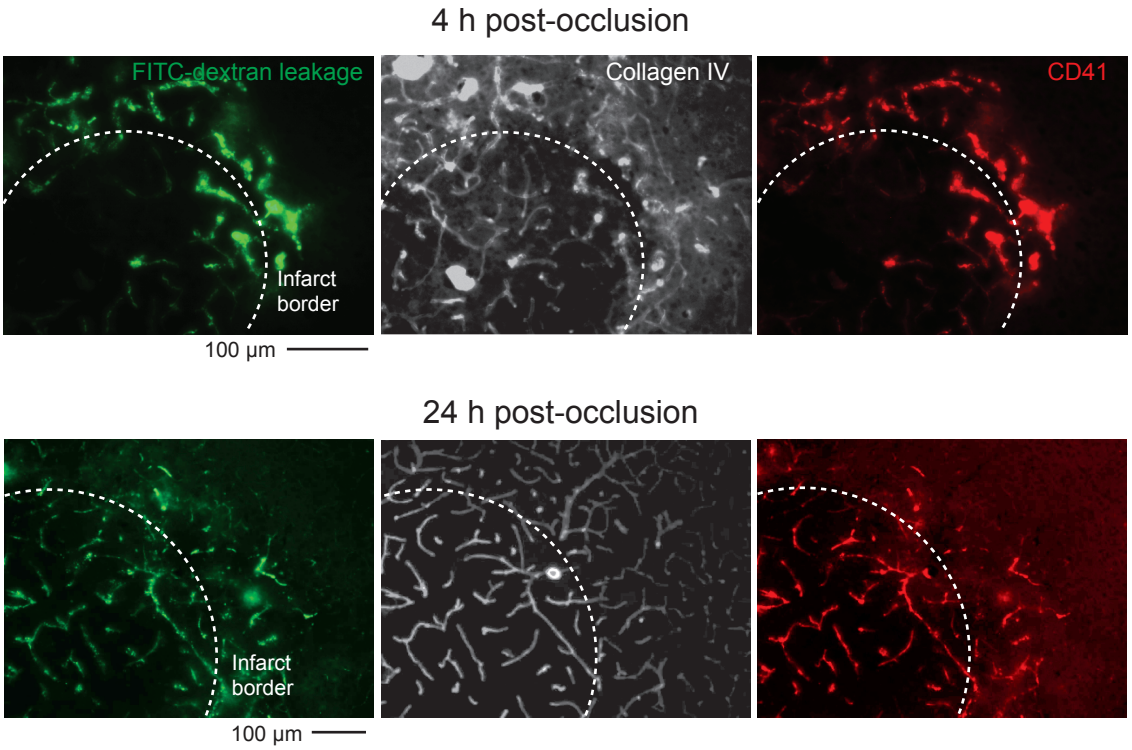

Figure S6. Taylor, Hui, Watson, Nie, Deardorff, Jensen, Helpern and Shih

Supplemental Material for "Microvascular basis for growth of small infarcts following occlusion of single penetrating arterioles in mouse cortex " by Zachary J. Taylor, Edward S. Hui, Ashley N. Watson, Xingju Nie, Rachael L. Deardorff, Jens H. Jensen, Joseph A. Helpern and Andy Y. Shih

Table S1. Systemic physiological measurements

N = 5 mice	**Pre-stroke**	**4 h post-stroke**	**8h post-stroke**
Heart rate (beats per min)	446 ± 30	438 ± 16	424 ± 30
Blood oxygen saturation (%)	96 ± 2	93 ± 3	94 ± 2